Final report for individual research grant

DFG-RFBR Cooperation: Joint German-Russian Project Proposals in all fields of science (funding period 2019-2021)

1 General Information

DFG reference number:	LO 310/17-1
Project number:	SCHU 1978/19-1
Project title:	Refractive dynamic tensor tomography: towards a holistic approach

Names and adresses of the applicants

Thomas Schuster, Prof. Dr. (German Principal Investigator)

Full Professor of Mathematics
Department of Mathematics, Saarland University
66123 Saarbrücken, Germany
Phone: ++49 681 302 57425
Email: thomas.schuster@num.uni-sb.de

Alfred K. Louis, Prof. Dr. (Co-Applicant, deceased 19 July 2024)

Full Professor of Mathematics

Former contact:
Department of Mathematics, Saarland University
66123 Saarbrücken, Germany
Phone: ++49 681 302 3018
Email: louis@num.uni-sb.de

Names of the cooperation partner

Evgeny Yu. Derevtsov, Prof. Dr. (Russian Principal Investigator)

Doctor of Science
Sobolev Institute of Mathematics SB RAS
630090 Novosibirsk, Russia
Phone: ++7 383 333 28 92
Email: dert@math.nsc.ru

2 Summary

English: Within the framework of this project significant advancements in tensor tomography across various settings have been achieved including static, dynamic, attenuated, and refractive cases. Generalized attenuated ray transforms for higher-order tensor fields were studied, where integral moments were explicitly calculated providing unique solutions to boundary value problems under certain smoothness conditions. Novel numerical methods, particularly using the approximate inverse, demonstrated accurate reconstructions for 2D vector and 2-tensor tomography from limited data. Furthermore, singular value decompositions for the underlying integral transforms have been computed and continuity estimates in Sobolev-Bochner spaces were derived. An alternative approach investigated tensor tomography as an inverse source problem for transport equations that emerge from the geodesic vector field. By adding a viscosity term, weak solutions were analyzed, proving unique existence under mild conditions on refractive indices and absorption coefficients. The adjoint of the dynamic ray transform was deduced leading to two different, equivalent representations. The integral representation proved computationally simpler, albeit requiring geodesic equation solutions for different initial values. As for the numerical implementations, we focused on the stationary case, employing a polar grid. Challenges included optimal grid sampling and handling singularities at the origin. Synthetic data tests validated numerical convergence for decreasing viscosity parameters. The error analysis revealed that the integral representation significantly outperforms PDE-based methods in view of computational efficiency while achieving comparable reconstruction accuracy. The reconstruction was performed using the attenuated Landweber method with Nesterov acceleration applied to both, the integral and PDE-based formulations. The integral operator method proved to be superior regarding efficiency leading to its exclusive use for the non-Euclidean case. Additional experiments analyzed the impact of noise and deviations from straight-line trajectories confirming improved accuracy by using refraction modeling, despite increased computational cost.

Deutsch: Im Rahmen des Projekts wurden signifikante Fortschritte auf dem Gebiet der Tensor-Tomographie erzielt für statische, dynamische, gedämpfte Settings und unter Einbeziehung von Beugungen. Es wurden verallgemeinerte gedämpfte Strahl-Transformationen für Tensorfelder höherer Ordnung untersucht und Integralmomente berechnet, wodurch eindeutige Lösbarkeit des zugrunde liegenden Randwertproblems unter bestimmten Glattheitsannahmen bewiesen werden konnte. Neuartige Lösungsmethoden, die zum Teil auf der approximativen Inversen basieren, führten zu exakten Rekonstruktionen für Vektor- und 2-Tensorfelder in zwei Dimensionen. Des Weiteren wurden Singulärwertzerlegungen für die entsprechenden Integraltransformationen hergeleitet und Stetigkeits-Abschätzungen in Sobolev-Bochner-Räumen bewiesen. In einem alternativen Ansatz wurde Tensor-Tomographie als inverses Quellproblem für Transportgleichungen untersucht, welche auf dem geodätischen Vektorfeld beruhen. Durch Addition eines Viskositätsterms war es möglich, die eindeutige Existenz schwacher Lösungen unter bestimmten, milden Bedingungen an den Absorptionskoeffizienten und den Brechungsindex nachzuweisen. Der zum Vorwärtsproblem gehörende adjungierte Operator der dynamischen Strahl-Transformation wurde hergeleitet und führte zu zwei unterschiedlichen, äquivalenten Darstellungen. Die Integraldarstellung erwies sich dabei als rechnerisch einfacher, obwohl sie mehrfache Lösungen der geodätischen Differentialgleichung für unterschiedliche Anfangswerte erforderte. Die numerische Implementierung der Verfahren konzentrierte sich auf den stationären Fall unter Verwendung von Polargittern. Die Herausforderungen bestanden im optimalen Gittersampling und der Behandlung von Singularitäten im Ursprung. Unter Verwendung sythetischer Testdaten wurde numerische Konvergenz des Verfahrens

für unterschiedliche Regularisierungs- und Viskositätsparameter nachgewiesen. Die numerische Validierung ergab, dass die Verfahren, welche Integraldarstellungen verwenden, den PDE-basierten Methoden hinsichtlich Effizienz deutlich überlegen waren bei gleicher Rekonstruktionsgenauigkeit. In beiden Fällen wurde die gedämpfte Landweber-Methode mit Nesterov-Beschleunigung für die Rekonstruktion angewendet. Dabei erwies sich die Methode basierend auf Intergaloperatoren als effizienter und wurde daher für den nicht-Euklidischen Fall ausschließlich eingesetzt. Weitere Tests widmeten sich den Untersuchungen des Einflusses von Rauschen in den Daten sowie der Ablenkung der Trajektorien weg von Geraden, wobei sich zeigte, dass die Einbeziehung von Beugungen in die Modellierung die Genauigkeit erhöht und die höheren Rechenzeiten dadurch aufwiegt.

3 Progress report

Preliminary remark: The research within this project was significantly influenced by the COVID-19 pandemic that arose in March 2020 and made in-person conferences, meetings and staff exchanges with our Russian partners impossible. Research meetings were held online exclusively.

The inverse problem of tensor tomography: Tensor tomography means the inverse problem of reconstructing a tensor field f from integral data $\mathcal{I}f$ where the integration is along geodesic curves of a given Riemannian manifold. In the simplest case, these are straight lines as in classical X-ray CT. We call $\mathcal{I}$ the longitudinal ray transform. Refractive dynamic tensor tomography (RDTT) takes time-dependence of the fields, absorption and refraction of the rays into account and represents one of the most general tomographic settings in this field. Analytic and numerical solution methods require the inclusion of diverse mathematical disciplines such as vector and tensor calculus, Riemannian geometry, applied functional analysis, partial differential equations (PDEs), integral geometry and the theory of operator equations. It inspires new interpretations of tomography problems as inverse source problems for transport equations from known information about their solutions.

The mathematical model of RDTT: According to Fermat's principle an ultrasound signal propagates along the path with shortest travel time. This implies, that we can interpret the ray as a geodesic curve associated with the Riemannian metric

$$g_{ij}(x) = n^2(x)\delta_{ij}, \quad 1 \le i, j \le N, \tag{1}$$

which is generated by the refractive index $n(x)$. With respect to this metric, rays within the medium do not longer propagate along straight lines, but along geodesic curves that solve the initial value problem

$$\ddot{\gamma}^k + \Gamma^k_{ij}(\gamma)\dot{\gamma}^i\dot{\gamma}^j = 0, \quad k = 1, \dots, N, \quad \gamma(0) = x, \quad \dot{\gamma}(0) = \xi, \tag{2}$$

where Γ^k_{ij} are the Christoffel symbols associated with the metric g. Given the initial position x and initial direction (tangential vector) ξ of propagation, the ray can be inferred unambiguously under the assumption of a sufficiently smooth refractive index $n(x)$ as a solution of (2). Let $f = f(x) = (f_{i_1,\dots,i_m}(x))$ be a tensor field of rank m supported in a bounded domain $M \subset \mathbb{R}^N$ ($N = 2, 3$), the task consists of computing f, or at least its solenoidal part f^s, from the attenuated longitudinal ray transform

$$[\mathcal{I}_\alpha f](x, \xi) = \int_{\tau_-(x,\xi)}^0 \langle f(\gamma_{x,\xi}(\tau)), \dot{\gamma}^m_{x,\xi}(\tau)\rangle \exp\left(-\int_\tau^0 \alpha(\gamma_{x,\xi}(\sigma), \dot{\gamma}_{x,\xi}(\sigma))\mathrm{d}\sigma\right)\mathrm{d}\tau. \tag{3}$$

Here, $\alpha \ge 0$ denotes the absorption coefficient and $\gamma_{x,\xi}$ is a geodesic curve in the compact Riemannian manifold (M, g) starting in $x \in \partial M$ at time $\tau = 0$ and moving in direction ξ which is a unit tangential

vector in the tangent space T_xM at x. By $\tau_\pm(x,\xi)$ we denote exit and entry time of the signal into the object. The parametrization is illustrated by figure 1.

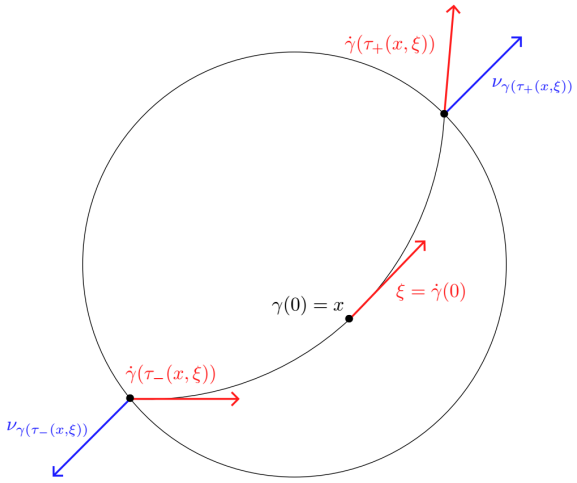

Figure 1: Sketch of a geodesic curve with parametrization γ

It can be shown (see, e.g., [1, 7]), that this problem is equivalent to computing the source term f in the transport equation

$$\mathcal{H}u(x,\xi)+\alpha u(x,\xi)=f\cdot\xi^m, \tag{4}$$

where $\mathcal{H}$ denotes the geodesic vector field corresponding to the metric g, $x\in M$, $\xi\in T_xM$ and $\xi^m=\xi\otimes\cdots\otimes\xi$ is the m-fold tensor product of ξ. Indeed, an extension of $u(x,\xi)=[\mathcal{I}_\alpha f](x,\xi)$ to the tangent bundle TM solves (4) and the generalized ray transform $\mathcal{I}_\alpha f$ therefore determines the boundary data of u. This formulation extends to dynamic settings of the ray transform for time-depending tensor fields f,

$$[\mathcal{I}_\alpha^d f](t,x,\xi)=\int_{\tau_-(x,\xi)}^0\langle f(t+\tau,\gamma_{x,\xi}(\tau)),\dot\gamma_{x,\xi}^m(\tau)\rangle\exp\left(-\int_\tau^0\alpha(\gamma_{x,\xi}(\sigma),\dot\gamma_{x,\xi}(\sigma))\mathrm{d}\sigma\right)\mathrm{d}\tau, \tag{5}$$

where an extension $u(t,x,\xi)=[\mathcal{I}_\alpha^d f](t,x,\xi)$ to $[0,T]\times TM$ solves

$$\Big(\frac{\partial}{\partial t}+\mathcal{H}+\alpha\Big)u(t,x,\xi)=f(t,x)\cdot\xi^m. \tag{6}$$

Without loss of generality, we assume that ξ is a unit vector with respect to the metric g. Under this assumption, equation (6) holds on the domain $[0,T]\times\Omega M$, where ΩM is defined as

$$\Omega M\coloneqq\{(x,\xi)\in TM\colon x\in M,\xi\in T_xM,\|\xi\|=1\}. \tag{7}$$

The boundary $\partial\Omega M$ can be decomposed into an inflow and an outflow boundary, given by

$$\partial_\pm\Omega M\coloneqq\{(x,\xi)\in\Omega M\colon x\in\partial M,\ \pm\langle\nu(x),\xi\rangle>0\}, \tag{8}$$

where $\nu(x)$ denotes the outward unit normal vector at $x\in\partial M$. This leads to the following boundary conditions:

$$u(t,x,\xi)=0, \qquad (x,\xi)\in\partial_-\Omega M, \tag{9}$$
$$u(t,x,\xi)=[\mathcal{I}_\alpha^d f](t,x,\xi), \qquad (x,\xi)\in\partial_+\Omega M. \tag{10}$$

For detailed proofs and further discussions, we refer to [DVS19, DVS21], where the expressions $f(x)\cdot\xi^m$ and $f(t,x)\cdot\xi^m$ have been extended to the more general settings $f(x,\xi)$ and $f(t,x,\xi)$, respectively. The general formulation (5) for time-depending tensor fields f covers a broad range of dynamic scenarios

depending on the underlying data sampling scheme and on the dynamic rate of f, resulting in two different time-scales for the data $u(t,\cdot)$ and the time-depending field $f(t,\cdot)$. Indeed, the acquisition of different data samples $u(x,\xi)$ itself takes already a considerable amount of time and thus needs to be suitably correlated to the time scale of the dynamics of f. Accounting for this aspect, the operator $\mathcal{I}_\alpha^d f$ from (5) reads

$$[\mathcal{I}_\alpha^d f](x,\xi) = \int_{\tau_-(x,\xi)}^0 \langle f(t(x,\xi),\gamma_{x,\xi}(\tau)), \dot\gamma_{x,\xi}^m(\tau)\rangle \exp\left(-\int_\tau^0 \alpha(\gamma_{x,\xi}(\sigma),\dot\gamma_{x,\xi}(\sigma))\mathrm{d}\sigma\right)\mathrm{d}\tau, \tag{11}$$

where $t(x,\xi)$ models the coupling of both time-scales. In the following, we provide an overview of our main achievements during the cooperation.

Achievements within this project: During this project, together with our cooperation partners from Sobolev Institute of Mathematics, Novosibirsk (Russia), deciding advances have been made towards a holistic approach to tensor tomography in fairly general settings (static / dynamic, including attenuation and refraction), which we summarize in the following.
In [DVS19, DVS21, DVS20, DVS++19] generalized attenuated ray transforms (GART) of higher order tensor fields have been considered for which integral moments could be calculated explicitly. For any order, they present the unique solution of a boundary value problem under certain smoothness conditions for α. The articles [LMP+20, ML20, SML19] deal with new numerical methods based on the method of approximate inverse for 2D vector and 2-tensor tomography problems from limited data. The solvers show good reconstruction results of the solenoidal as well as potential parts. Inversion formulas for vector and tensor ray transforms were derived in [L22]. In [5, 6] the dynamic longitudinal, mixed and transverse ray transforms acting on symmetric 2-tensor fields are investigated. It was possible to prove mathematical properties of the integral operators and the singular value decomposition could be constructed. In particular, concerning the ray transform as discussed in (5), continuity estimations within suitable Sobolev-Bochner spaces have been established, we refer to [V24] for further details. In [L24], the last article Alfred Louis published in his lifetime, a unified approach to inversion formulas for longitudinal and transverse ray transforms of vector and tensor fields has been deduced.
An alternative approach considers general tensor tomography problems as inverse source problems for corresponding transport equations by computing f from (4), (6) where (initial-) boundary values are given via the ray transforms $\mathcal{I}_\alpha f$ (3), $\mathcal{I}_\alpha^d f$ (5). The existence and uniqueness of weak solutions have been investigated. Existence is obvious, since an extension of $u(x,\xi) = \mathcal{I}_\alpha f$ to the entire tangent bundle TM solves (4) and the analogue is valid for (6). Uniqueness however does not hold true, since the corresponding bilinear forms are not H^1-coercive. As a remedy, we turn over to viscosity solutions (cf. [2]) by adding a multiple of the Laplacian, $-\varepsilon\Delta$, for some small parameter $\varepsilon > 0$ to the left side of (4) resulting in

$$-\varepsilon\Delta u_\varepsilon(x,\xi) + \mathcal{H}u_\varepsilon(x,\xi) + \alpha u_\varepsilon(x,\xi) = f(x)\cdot\xi^m, \qquad \varepsilon > 0. \tag{12}$$

We succeeded to prove unique existence of weak solutins for (12) for arbitrary $\varepsilon > 0$ under a certain, mild additional condition to the refractive index $n(x)$ and the absorption coefficient α,

$$\sup_{x\in M} \frac{|\nabla n(x)|}{n(x)} < \alpha_0, \tag{13}$$

where we assume $\alpha(x,\xi) \geq \alpha_0 > 0$ a.e. Assumption (13) means that the refractive index may vary only slightly in space. An analogue holds true for the dynamic case. The details of the proofs can be found in the article by Vierus and Schuster [VS22]. The proofs are valid even in settings, where $f\cdot\xi^m$ at the right-hand side of (12) is replaced by general $f(x,\xi)$ and $f(t,x,\xi)$, respectively.

The results are of utmost importance for solving tensor tomography problems in fairly general settings, since these can be interpreted as inverse source problems for transport equations. In fact, the inverse problem of DRTT using PDEs reads as $\mathcal{S}_\alpha^{\varepsilon,d} f = h$, where the forward operator decomposes as $\mathcal{S}_\alpha^{\varepsilon,d} = \gamma_+ \circ \mathcal{F}_\alpha^{\varepsilon,d}$ with $\mathcal{F}_\alpha^{\varepsilon,d}$ as the parameter-to-solution map, and γ_+ as the trace operator, restricting the solution u_ε to the boundary $\partial_+ \Omega M$. The adjoint problem is given by

$$[(\mathcal{S}_\alpha^d)^* h](t,x) = \int_{\Omega_x M} w(t,x,\xi)\xi^m \,\mathrm{d}\sigma_+(\xi),$$

where w is the weak solution of the terminal boundary value problem

$$-\frac{\partial w}{\partial t} - \mathcal{H} w + (\alpha + \Xi_n)\, w = 0, \qquad t \in [0,T],\ (x,\xi) \in \Omega M,$$

$$\begin{aligned}
&w(T,x,\xi) = 0, \qquad (x,\xi) \in \Omega M \\
&w(t,x,\xi) = \frac{h(x,\xi)}{\langle \nu_x, \xi \rangle}, \quad (x,\xi) \in \partial_+ \Omega M \\
&w(t,x,\xi) = k_h(x,\xi) \exp\Big(- \int_0^{\tau_+(x,\xi)} (\alpha + \Xi_n)(\gamma_{x,\xi}(\tilde\tau), \dot\gamma_{x,\xi}(\tilde\tau)) \mathrm{d}\tilde\tau \Big), \quad (x,\xi) \in \partial_- \Omega M
\end{aligned}$$

with

$$k_h(t,x,\xi) = \frac{h(t + \tau_+(x,\xi)\gamma_{x,\xi}(\tau_+(x,\xi)), \dot\gamma_{x,\xi}(\tau_+(x,\xi)))}{\langle \nu_{\gamma_{x,\xi}(\tau_+(x,\xi))}, \dot\gamma_{x,\xi}(\tau_+(x,\xi)) \rangle}.$$

For this problem, unique weak solvability could be proven in [V24] given the same condition (13). We applied the method of characteristics to this problem, obtaining a solution w along a geodesic curve, represented by

$$w(t,x,\xi) = k_h(t,x,\xi) \exp\Big(- \int_0^{\tau_+(x,\xi)} (\alpha + \Xi_n)(\gamma_{x,\xi}(\tilde\tau), \dot\gamma_{x,\xi}(\tilde\tau)) \mathrm{d}\tilde\tau \Big).$$

The adjoint operator of $\mathcal{I}_\alpha^d$ is then of backprojection type,

$$[(\mathcal{I}_\alpha^d)^* h](t,x) = \int_{\Omega_x M} w(t,x,\xi)\xi^m \,\mathrm{d}\sigma_+(\xi).$$

As a consequence, we obtain two different representations for describing both, the forward and adjoint operators. The main advantage of the integral representation is its fairly simple implementation. However, each evaluation point, which is required for approximating the integral, necessitates solving the geodesic equation (2) for different initial values x, ξ, and, thus, increases computational complexity. Regarding the numerical implementation, we confined to the stationary case and employed a polar grid and, hence, payed tribute to the radial symmetry of the problem. This required overcoming two key challenges: The first was the determination of the optimal ratio between the number of radial and angular grid points to ensure optimal performance. Through multiple tests, we found that the best ratio between angles P and radii R is approximately $P \approx \pi R$, a sampling condition which is well known from computerized tomography [4]. This ensures that the length of the straight grid lines is comparable to the average length of the curved segments, in analogy to the Cartesian case. The second challenge was to address the singularity of the gradient and Laplacian at the origin. Regarding the gradient, which consists of first radial derivatives, we exclusively used forward differences, particularly due to the structure of the innermost circle of the mesh. Addressing the singularity in the second derivatives required a more refined approach. Specifically, for approximating the second radial derivative at grid points $x_{1,p}$, where $p = 1, \ldots, P$, on the inner circle, we selected $x_{1,p+\frac{P}{2}}$ as the third node and adjusted the finite difference weights accordingly based on the Taylor expansion, see figure 2.

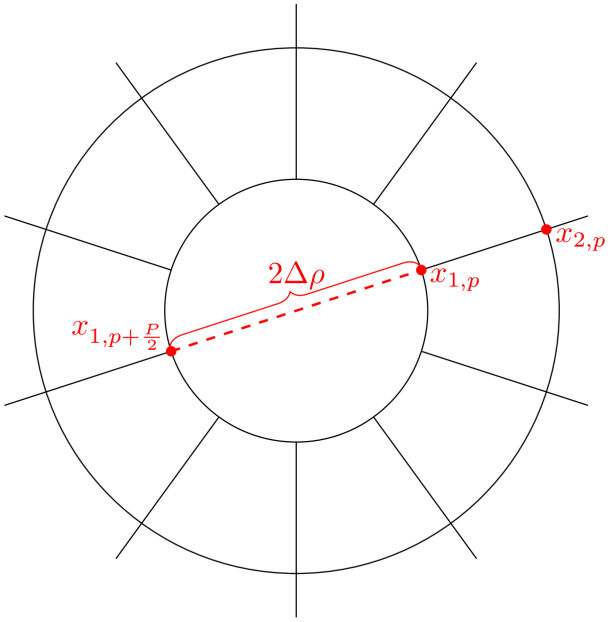

Figure 2: Nodes for approximating $\frac{\partial^2 w}{\partial r^2}(x_{1,p})$

As an example, we generated synthetic measurement data using the integral transform $\mathcal{I}_\alpha$ and computed the solution of the transport equation for various values of ε. This allowed us to demonstrate the numerical convergence of the solutions as $\varepsilon \to 0$. To determine, which approach to operator selection offers the most advantages, we specified particularly simple 2D vector fields f_i for our analysis. As for the homogeneous case (i.e., with a constant refractive index), we were able to compute the integral data $\mathcal{I}_\alpha f$ analytically. As measures for the accuracy of the adjoint operators, we selected the following error metrics

$$\mathrm{err}_f(\mathcal{I}_\alpha^*) = \frac{|\langle \mathcal{I}_\alpha f, \mathcal{I}_\alpha f\rangle - \langle f, \mathcal{I}_\alpha^* \mathcal{I}_\alpha f\rangle|}{\langle \mathcal{I}_\alpha f, \mathcal{I}_\alpha f\rangle}, \qquad \mathrm{err}_f((\mathcal{S}_\alpha^\varepsilon)^*) = \frac{|\langle \mathcal{I}_\alpha f, \mathcal{I}_\alpha f\rangle - \langle f, (\mathcal{S}_\alpha^\varepsilon)^* \mathcal{I}_\alpha f\rangle|}{\langle \mathcal{I}_\alpha f, \mathcal{I}_\alpha f\rangle}.$$

This means the better the approximation is, the smaller the corresponding errors. We evaluated them given the field $f(x) = (x_1, -x_2)^\top$. The results are depicted in figure 3.

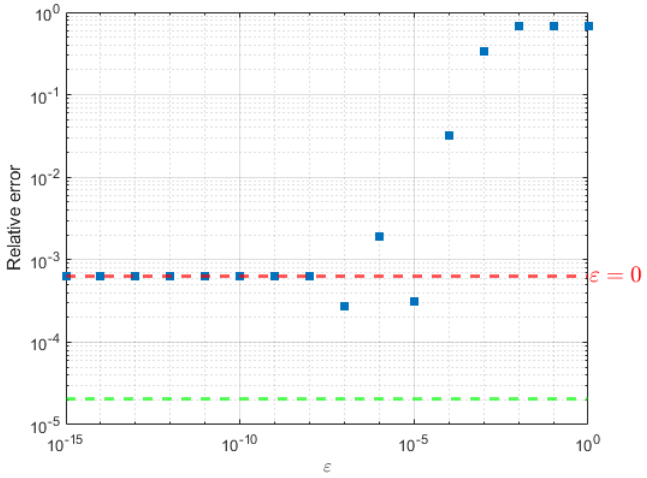

Figure 3: $\mathrm{err}_f((\mathcal{S}_0^\varepsilon)^*)$ for $\varepsilon > 0$, $\mathrm{err}_f((\mathcal{S}_0^0)^*)$ and $\mathrm{err}_f(\mathcal{I}_0^*)$ for $f(x) = (x_1, -x_2)^\top$

In this example, it can be clearly observed that as ε decreases, the error $\mathrm{err}_f((\mathcal{S}_\alpha^\varepsilon)^*)$ converges to the value for $\varepsilon = 0$. Moreover, it is also evident that significantly better results can be achieved using the

integral operator. For reconstruction, we investigated both approaches using an attenuated Landweber iteration (cf. [3]), incorporating a Nesterov scheme for acceleration,

$$z_{k+1} = f_k + \frac{k-1}{k+2}(f_k - f_{k-1}),$$
$$f_{k+1} = z_{k+1} - \omega \mathcal{I}_\alpha^*(\mathcal{I}_\alpha z_{k+1} - h^\delta), \qquad k = 0, 1, \dots.$$

for noisy data h^δ. The same method is used for $\mathcal{I}_\alpha$ replaced by $\mathcal{S}_\alpha^\varepsilon$. As can be seen from table 1 the relative errors for both variants of the adjoints are comparable, but computation time differs tremendously (roughly by a factor of 35). This is why we decided to only use $\mathcal{I}_\alpha$ and $\mathcal{I}_\alpha^*$ for non-Euclidean metrics. In Figure 4, we illustrated the impact of noise on the reconstruction in the case of refractive indices that slightly deviate from a constant value and satisfy condition (13). We used the optimal grid consisting of 34×106 spatial points x and 106 directions ξ. It is evident that even for larger noise levels, the absolute error in each pixel remains relatively small.

Choice of adjoint	Noise level	Relative error	Run time
$\mathcal{I}_0^*$	3%	1.30%	5 min 5 s
	10%	3.39%	3 min 32 s
$\mathcal{S}_0^*$	3%	1.27%	178 min 53 s
	10%	3.34%	124 min 25 s

Table 1: Computation time for the adjoint operators

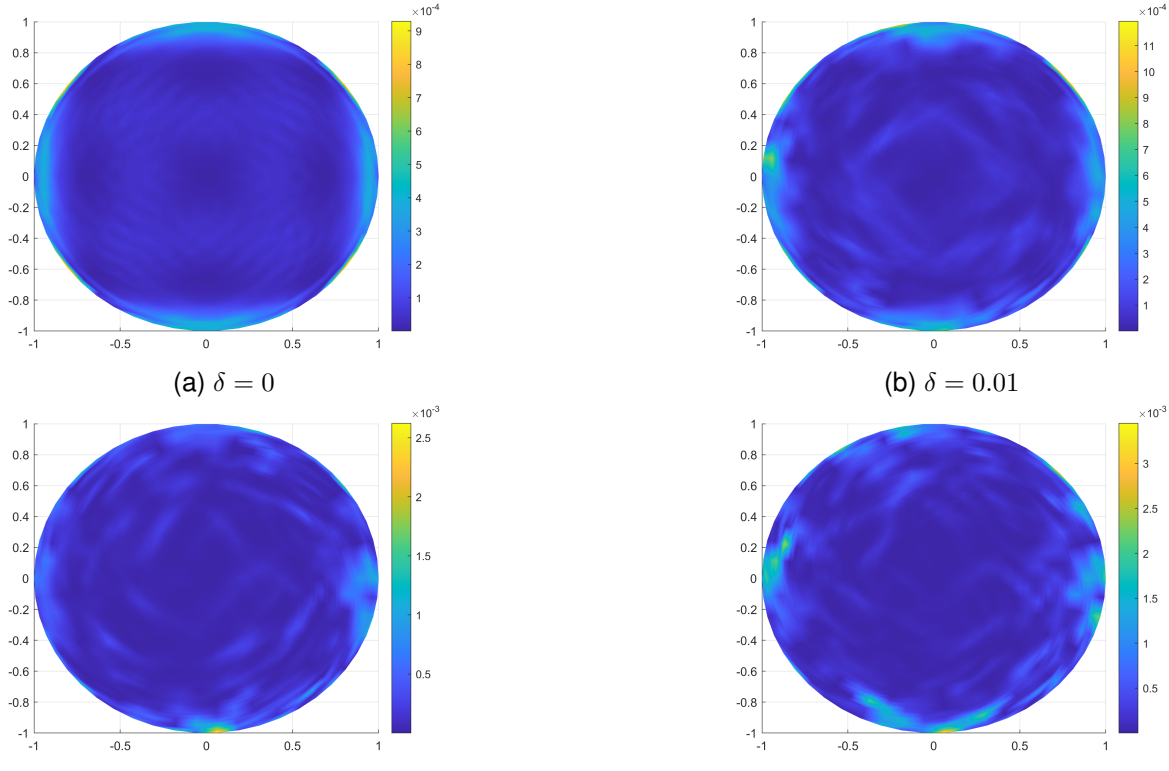

(a) $\delta = 0$ (b) $\delta = 0.01$

(c) $\delta = 0.02$ (d) $\delta = 0.03$

Figure 4: Absolute error in reconstruction of f with $\mathcal{I}_{0.01}^*$ in non-Euclidean setting for $(R, P, Q) = (34, 106, 106)$ and $n(x) = 0.002|x|^2 + \frac{4}{3}$ and different noise levels $\delta > 0$

Finally, we investigated whether incorporating small deviations from straight lines into our model really pays, given the significantly increased computational effort. We simulated measurement data using

the full model and attempted to reconstruct f comparing whether the error decreases if refraction is taken into account for the reconstruction. Table 2 proves that the L^2-error increases by a factor of 5 if the reconstruction is done under the assumption of straight-line propagation, although refraction is apparent. At the same time, the computational costs are significantly larger in case of non-Euclidean geometries. The reason for the latter comes from the necessity to solve the geodesic equation (2) for different initial conditions in every iteration for each evaluation of a geodesic integral.

Noise level	Attenuation	Refraction	L^2-error	Run time
0	0.01	no	0.0555	21 min 21 s
0	0.01	yes	0.0132	52 min 2 s
0.01	0.01	no	0.0559	10 min 55 s
0.01	0.01	yes	0.0144	69 min 9 s

Table 2: Reconstruction of f with Euclidean and non-Euclidean model

The software developed in this project is publicly available under `https://github.com/tschus71/RDTT`.

A series of lectures have been held to disseminate the achievements of the research performed within the project:

- NUMTA Conference in Le Castella Village, Italy (2019)
- ESI Workshop *Tomographic Reconstructions and their Startling Applications* in Vienna (2021, online)
- 2nd Alps-Adriatic Workshop in Klagenfurt, Austria (2021)
- International Conference on Inverse Problems: Modeling and Simulation (IPMS) in Malta (2022)
- Workshop *Tomographic Inverse Problems* in Oberwolfach (2023)
- 3rd Alps-Adriatic Workshop in Klagenfurt, Austria (2023)
- GIP Annual Meeting in Siegen (2023)

Bibliography

[1] G. Ainsworth and Y.M. Assylbekov. On the range of the attenuated magnetic ray transform for connections and Higgs fields. *arXiv preprint arXiv:1311.4582*, 2013.

[2] M.G. Crandall and P.-L. Lions. Viscosity solutions of Hamilton-Jacobi equations. *Transactions of the American mathematical society*, 277(1):1–42, 1983.

[3] L. Landweber. An iteration formula for Fredholm integral equations of the first kind. *Amer. J. Math.*, 73:615–624, 1951.

[4] Frank Natterer. *The Mathematics of Computerized Tomography*. SIAM, 2001.

[5] Anna P Polyakova, Ivan E Svetov, and Bernadette N Hahn. The singular value decomposition of the operators of the dynamic ray transforms acting on 2D vector fields. In *International Conference on Numerical Computations: Theory and Algorithms*, pages 446–453. Springer, 2019.

[6] A.P. Polyakova and B. Hahn. A solution of the dynamic two-dimensional 2-tensor tomography problem using the svd-method. In *International Conference ''Frontier in Mathematics and Computer Science"*, 2020.

[7] V.A. Sharafutdinov. *Integral Geometry of Tensor Fields*. VSP, Utrecht, 1994.

(References not related to the project are quoted by numbers.)

4 Published Project Results

4.1 Publication with scientific quality assurance

[DVS20] E.Y. Derevtsov, Y.S. Volkov and T. Schuster. Integral operators at settings and investigations of tensor tomography problems. *Continuum Mechanics, Applied Mathematics and Scientific Computing: Godunov's Legacy*, 111-117, doi:10.1007/978-3-030-38870-6_15, 2020.

[DVS21] E.Y. Derevtsov, Y.S. Volkov and T. Schuster. Generalized attenuated ray transforms and their integral angular moments. *Applied Mathematics and Computation*, 409, doi:10.1016/j.amc.2020.125494, 2021.

[L22] A.K. Louis. Inversion formulae for ray transforms in vector and tensor tomography. *Inverse Problems*, 38, ID 065008, doi:10.1088/1361-6420/ad5d0e, 2022.

[LMP+20] A.K. Louis, S.V. Maltseva, A.P. Polyakova, T. Schuster and I.E. Svetov. On solving slice-by-slice three-dimensional 2-tensor tomography problems using the method of approximate inverse. *Journal of Physics: Conference Series. IOP Publishing*, doi:10.1088/1742-6596/1715/1/012036, 2020.

[MSL21] S.V. Maltseva and I.E. Svetov and A.K. Louis. An iterative algorithm for reconstruction a 2D vector field by its limited-angle ray transform. *Journal of Physics: Conference Series*, 1715(1), doi:10.1088/1742-6596/1715/1/012037, 2021.

[VS22] L. Vierus and T. Schuster. Well-defined forward operators in dynamic diffractive tensor tomography using viscosity solutions of transport equations. *Electronic Transactions on Numerical Analysis (ETNA)*, 57:80-100, doi:10.48550/arXiv.2111.05722, 2022.

[L24] A.K. Louis. A unified approach to inversion formulae for vector and tensor ray and radon transforms and the Natterer inequality. *Inverse Problems*, 40, ID 085007, doi:10.1088/1361-6420/ad5d0e, 2024.

4.2 Other publications and published results

[DVS19] E.Y. Derevtsov, Y.S. Volkov and T. Schuster. Differential equations and uniqueness theorems for the generalized attenuated ray transforms of tensor fields. *International Conference on Numerical Computations: Theory and Algorithms*, 97-111, doi:10.1007/978-3-030-40616-5_8, 2019.

[DVS++19] E. Derevtsov, Y. Volkov and T. Schuster. Integral and differential operators as the tools of integral geometry and tomography. *Numerical Computations: Theory and Algorithms NUMTA 2019*, `https://re.public.polimi.it/retrieve/e0c31c0f-15d5-4599-e053-1705fe0aef77/Book_NUMTA2019.pdf#page=243`, 2019.

[ML20] S.V. Maltseva, I.E. Svetov and A.K. Louis. An iterative algorithm for reconstructing a 2D vector field by its limited-angle ray transform. *Journal of Physics: Conference Series*, 1715, doi:10.1088/1742-6596/1715/1/012037, 2021.

[SML19] I.E. Svetov and S.V. Maltseva and A.K. Louis. The method of approximate inverse in slice-by-slice vector tomography problems. *International Conference on Numerical Computations: Theory and Algorithms*, 487-494, doi:10.1007/978-3-030-40616-5_47, 2019.

[V24] L. Vierus. Dynamic refractive tensor field tomography as an inverse problem for a transport equation. *Doctoral thesis, Saarland University Saarbrücken*, http://dx.doi.org/10.22028/D291-43551, 2024.

4.3 Patents (applied for an granted)

None.